The Mechanics of Seated and Nonseated Cycling at Very-High-Power Output: A Joint-Level Analysis

ROSS D. WILKINSON, GLEN A. LICHTWARK, and ANDREW G. CRESSWELL

School of Human Movement and Nutrition Sciences, Centre for Sensorimotor Performance, The University of Queensland, St Lucia, Queensland, AUSTRALIA

ABSTRACT

WILKINSON, R. D., G. A. LICHTWARK, and A. G. CRESSWELL. The Mechanics of Seated and Nonseated Cycling at Very-High-Power Output: A Joint-Level Analysis. *Med. Sci. Sports Exerc.*, Vol. 52, No. 7, pp. 1585–1594, 2020. Cyclists frequently use a nonseated posture when accelerating, climbing steep hills, and sprinting; yet, the biomechanical difference between seated and nonseated cycling remains unclear. **Purpose:** This study aimed to test the effects of posture (seated and nonseated) and cadence (70 and 120 rpm) on joint power contributions, effective mechanical advantage, and muscle activations within the leg during very-high-power output cycling. **Methods:** Fifteen male participants rode on an instrumented ergometer at 50% of their individualized instantaneous maximal power (10.74 ± 1.99 W·kg^{-1}; above the reported threshold for seated to nonseated transition) in different postures (seated and nonseated) and at different cadences (70 and 120 rpm) while leg muscle activity, full-body motion capture, and crank radial and tangential forces were recorded. A scaled, full-body model was used to solve inverse kinematics and inverse dynamics to determine joint displacements and net joint moments. Statistical comparisons were made using a two-way repeated-measures ANOVA (posture–cadence). **Results:** There were significant main effects of posture and cadence on joint power contributions. A key finding was that the nonseated posture increased negative power at the knee, with an associated significant decrease of net power at the knee. The contribution of knee power decreased by 15% at both 70 and 120 rpm (~0.8 W·kg^{-1}) when nonseated compared with seated. Subsequently, hip power and ankle power contributions were significantly higher when nonseated compared with seated at both cadences. In both postures, knee power was 9% lower at 120 rpm compared with 70 rpm (~0.4 W·kg^{-1}). **Conclusion:** These results evidenced that the contribution of knee joint power to leg power was reduced by switching from a seated to nonseated posture during very-high-power output cycling; however, the size of the reduction is cadence dependent. **Key Words:** CADENCE, JOINT POWER, STANDING, MECHANICAL ADVANTAGE, ELECTROMYOGRAPHY

Cyclists often transition from a seated to a nonseated posture during short, intensive bouts of climbing, accelerating, and sprinting (1). An increased understanding of the biomechanical differences between the seated and the nonseated postures has practical importance for cycling performance and equipment design (2), as well as injury prevention and rehabilitation (3). The nonseated posture is typified by cyclists raising their pelvis off the saddle, which results in more extended hip and knee angles, an altered direction of the resultant crank force (4), and an effective use of body mass to generate positive power at the crank during the downstroke (5). Although it is known that the nonseated posture is more effective than the seated posture for maximal power production (6,7), cyclists often transition off the saddle well before their limit of power production is reached (1,8). For example, using an incremental testing protocol within a laboratory setting, it was determined that noncyclists spontaneously transitioned to a nonseated posture at 568 ± 93 W (7.9 ± 1.4 W·kg^{-1}) when pedaling at a cadence of 90 rpm (1), well below the 6-s maximal power production measured in a similar untrained population of 813 ± 137 W (12.43 ± 1.34 W·kg^{-1}) (9).

Field testing (2) has shown that competitive cyclists can increase their time to exhaustion during uphill cycling by using the nonseated posture when the required power output is at or above 419 ± 30 W (5.6 ± 0.4 W·kg^{-1}). In the same study, it was shown that preferred cadence decreased from 92 ± 2 rpm when seated to 74 ± 3 rpm when nonseated. This preference for a lower cadence when nonseated implies that cyclists favor generating power at the crank by increasing crank torque and reducing crank angular velocity. Thus, if we assume the range of motion at each leg joint to be similar between postures, possible benefits of the transition could be that it alters the conditions under which muscles generate power and allows cyclists

Address for correspondence: Ross D. Wilkinson, B.A., Exercise and Sports Science, School of Human Movement and Nutrition Sciences Brisbane, The University of Queensland, QLD, 4072, Australia; E-mail: ross.wilkinson@uqconnect.edu.au.
Submitted for publication December 2018.
Accepted for publication January 2020.
Supplemental digital content is available for this article. Direct URL citations appear in the printed text and are provided in the HTML and PDF versions of this article on the journal's Web site (www.acsm-msse.org).

0195-9131/20/5207-1585/0
MEDICINE & SCIENCE IN SPORTS & EXERCISE®

DOI: 10.1249/MSS.0000000000002285

APPLIED SCIENCES

to redistribute power requirements to different muscles. Currently, no feasible methods exist to directly measure this redistribution at a muscular level; however, the integration of inverse dynamics and EMG may provide indirect evidence of these changes.

Joint-level analyses of seated cycling have shown that the distribution of leg power among the hip, knee, and ankle is sensitive to the torque and angular velocity demands at the crank (10,11). For example, Elmer et al. (10) reported that as net crank power increased from 250 to 850 W at a constant cadence of 90 rpm (i.e., increasing torque demand), the contribution of knee extension power decreased, whereas the contribution of knee flexion power increased. A similar analysis of seated maximal sprint cycling by McDaniel et al. (11) found that as cadence increased from 60 to 180 rpm, the contribution of hip extension power and knee flexion power increased, whereas the contribution of knee extension power did not change. These findings provide an indication of how joint power is likely to be redistributed in response to changes in power output and cadence; however, it is not known whether a similar redistribution of joint power will occur when nonseated.

EMG analyses have provided insight into the sources of power generation during nonseated cycling (12,13); however, fundamental mechanical differences between the seated and the nonseated postures remain unresolved. These gaps exist primarily because previous research has focused on either performance (2,7) or physiological economy differences (6,14,15) between the two postures. Thus, biomechanical assessments of the nonseated posture remain incomplete and allow only speculation of the underlying mechanical interaction of muscles and body segments. It seems likely that the kinematic differences between the seated and the nonseated postures, notably the anterior shift in the rider's center of mass and more extended hip and knee position, will affect the pattern of power production and absorption within the leg, especially at the knee. Yet to date, no study has determined whether the distribution of leg power among the hip, knee, and ankle differs between the seated and the nonseated postures.

The present study was designed to compare the distribution of joint powers between seated and nonseated postures during very-high-power output cycling at two different cadences. Effective mechanical advantage (EMA) and muscle activity in the right leg was also compared between postures under these same cadence and power conditions. First, we hypothesized that at a constant external power output, the net contribution of knee power to leg power (sum of ankle, knee, and hip power) would be lower in the nonseated compared with seated posture. Second, we hypothesized that the net contribution of knee power to leg power would be cadence dependent in the nonseated posture.

METHODS

Participants

Fifteen active and healthy males (mean ± SD, age = 30 ± 8 yr, height = 1.79 ± 0.05 m, mass = 74.4 ± 8.5 kg) volunteered to be participants for this study. The athletic background of the participant group was varied. Eight of the participants were cyclists who competed weekly at club level, whereas the remainder regularly engaged in a variety of competitive or recreational sports. All participants gave their written informed consent before participating in this study according to the procedures approved by the Human Ethics Committee of The University of Queensland and in accordance with the general principles expressed in the Declaration of Helsinki.

Experimental Protocol

Participants performed five 3-s all-out seated sprints to determine their peak instantaneous maximal power ($P_{max.i}$) followed by four submaximal trials at 50% of their individual $P_{max.i}$ under different combinations of posture (seated or nonseated) and cadence (70 or 120 rpm), outlined below.

Ergometer setup. Once the participants were deemed fit for testing, their body mass, height, inside leg length, torso length, arm length, and shoe size were measured. These measures were then used to fit the participants to the cycling ergometer, which was used for all trials (Excalibur Sport, Lode BV, Groningen, The Netherlands). Seat tube angle was standardized to 73° with respect to horizontal position, and knee angle was standardized to 150° of extension when the right pedal was at its lowest position. This angle was measured using a goniometer with the participant in a static, seated posture on the ergometer. Knee angle was determined from the bisection of two lines connecting markers placed on the greater trochanter, lateral femoral condyle, and lateral malleolus. The saddle height and the fore-aft position of the saddle were incrementally adjusted until the desired combination of knee angle and seat tube angle was achieved. Torso angle was standardized to 70°, with arms slightly bent at the elbow and hands placed in the drops of the handlebar. Torso angle was defined with respect to horizontal position by the line connecting markers placed on the acromion process and greater trochanter. Some minor adjustments to this fitting were allowed based on participant preference. Crank length was constant at 175 mm. Participants wore a standardized model of cleated cycling shoe (SH-R070; Shimano, Osaka, Japan) that clipped into the pedals (SH-R540, Shimano).

Maximal power output test. Participants began with a 5-min cycling warm-up at 100 W at their preferred cadence. Participants then performed five maximal sprints of 3-s duration in a seated posture to determine their individual $P_{max.i}$. The ergometer was set to "linear" mode, which ensured that power was coupled to cadence. It was expected that participants would achieve $P_{max.i}$ at a cadence of approximately 120 rpm (16–18). Thus, the linear resistance was increased or decreased for each subsequent trial based on whether the participant achieved a peak cadence above or below 120 rpm. $P_{max.i}$ was successfully determined within five trials for all participants and was calculated as the highest "instantaneous" power that occurred during a crank cycle. Participants were given 3 min of rest between trials to reduce any potential fatigue

effects. Note that peak instantaneous maximal power ($P_{max.i}$) was used to individualize the mean power output for the submaximal trials, as opposed to the mean maximal power over a complete crank cycle ($P_{max.m}$), which is more commonly reported (18).

Submaximal trials. A 20-min period of rest was given after the maximal power output test before commencing the four submaximal trials. The constant power output and cadence (70 or 120 rpm) conditions for the submaximal trials were chosen with the intention to create two scenarios where cyclists would prefer to ride in a nonseated position. This assumption was based on the reported seated to nonseated transition power at 90 rpm (1), and that this transition power is dependent on the amount of torque required per crank cycle. Thus, the power output had to be high enough for riders to still want to ride off the saddle at 120 rpm, but low enough that it was still achievable at 70 rpm in both postures. Pilot testing revealed that 50% of individual $P_{max.i}$ measured at approximately 120 rpm would be appropriate for this purpose. The two cadence conditions of 70 and 120 rpm were chosen primarily to provide a contrast in the amount of torque required per cycle; however, they also happen to be approximately equal to preferred cadences used during climbing (19) and sprinting (16), respectively. It should be noted that the selected power output and cadences were not intended to simulate the exact conditions of sprinting or climbing. Participants performed the combinations of posture and cadence in a randomized order and were required to maintain the target cadence and power output for a minimum period of 10 s. The ergometer was set to "hyperbolic" mode, which ensured that power output remained constant independent of cadence; thus, riders were required to maintain the specific set cadences using feedback from the visual display on the ergometer. To test for the presence of any exercise-induced fatigue, an additional 3-s maximal sprint was performed after the submaximal trials. Inclusion required the participants to be able to match (±5%) their previously tested $P_{max.i}$ in this additional trial. Kinematics, kinetics, and EMG were recorded during the submaximal trials.

Data Collection

All analog signals were acquired using a 16-bit analog-to-digital (A/D) conversion board (USB-2533; Measurement Computing Corporation, Norton, MA) using Qualisys Track Manager software (Qualisys AB, Gothenburg, Sweden).

Motion capture. An eight camera, optoelectronic motion capture system (Oqus, Qualisys, AB, Sweden) was used to measure the 3D position of 45 passive reflective markers at 200 Hz. Markers were secured using double-sided tape over the suprasternal notch, vertebrae C7, sacrum, and bilaterally over the acromion processes, lateral epicondyles of the humerus, styloid processes of the radius, iliac crests, anterior superior iliac spines, posterior superior iliac spines, greater trochanters, medial and lateral condyles of the femur, medial and lateral malleoli, calcanei, heads of the first and fifth metatarsals, and the second distal phalanxes (marker placements are shown in Fig. 1). Lightweight rigid clusters of four markers were also secured bilaterally to the lateral midthighs and lateral midshanks using double-sided tape and self-adhesive bandage. Before the submaximal trials, marker positions were captured with the participant standing in a standard anatomical posture. This static trial was later used for scaling purposes during data processing. The heading (sc. yaw) angle of the ergometer was determined relative to the motion capture global coordinate system by placing two passive reflective markers on the rear support legs of the ergometer. These markers were used to establish a local coordinate system for the ergometer, which accounted for any discrepancy with the global coordinate system between trials.

Crank angle and forces. Tangential and radial forces at the left and right crank as well as crank angle were recorded at

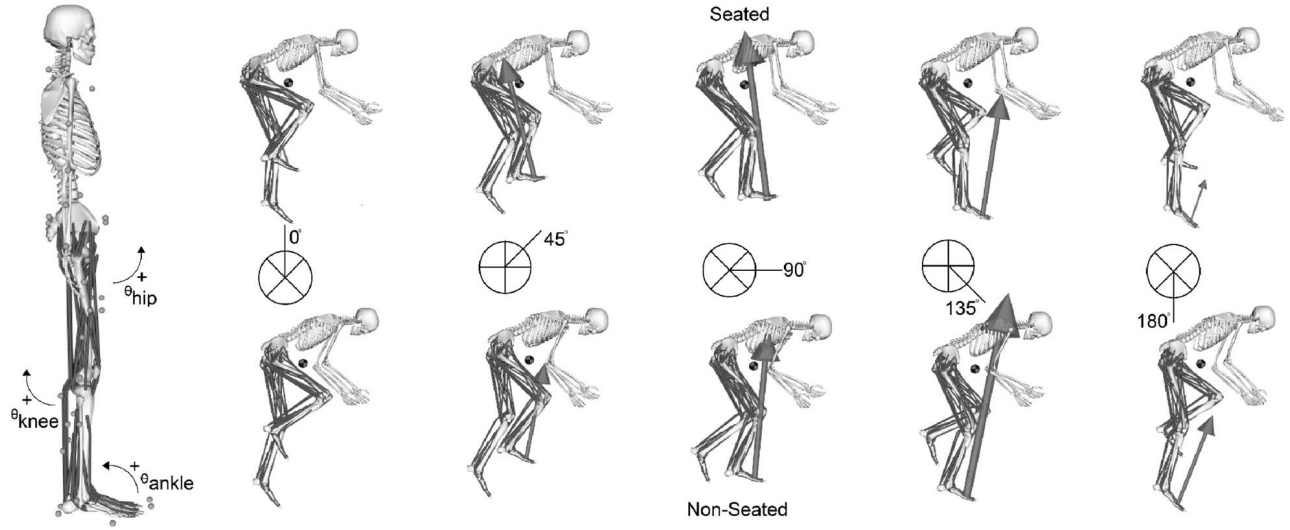

FIGURE 1—Sagittal plane images of a representative participant during a static trial (*left*) showing the definition of hip, knee, and ankle joint angles and marker positions, and during seated and nonseated cycling at 70 rpm for five selected crank positions during the downstroke (0°, 45°, 90°, 135°, and 180°). Arrows represent the magnitude and direction of the resultant crank reaction force vector. *Gray* and *black circle* represents the participant's center of mass position. NB: The clockwise shift in force production when nonseated compared with seated.

100 Hz using precalibrated, wireless, instrumented cranks (Axis; SWIFT Performance, Brisbane, Australia). Digital signals were transmitted wirelessly to a base receiver and then converted into an analog signal through the A/D Board. The digital sampling frequencies of the crank (100 Hz) and EMG (2 kHz) were matched to the motion capture (200 Hz) sampling frequency using the internal sampling factor within the Qualisys Track Manager software. A multiaxis, dynamic calibration of each crank was performed in house by the fabricating company (Swift Performance). In addition to and before testing, voltage offsets for tangential and radial force signals were determined by hanging a known mass of 2.5 kg from each pedal spindle with the cranks in a horizontal and vertical position, which allowed any discrepancy in the offset to be removed postprocessing. The crank angle signal was zeroed with the right crank at top dead center.

EMG. Surface EMG signals of gluteus maximus (GMax), rectus femoris (RF), long head of biceps femoris (BF), vastus lateralis (VL), gastrocnemius medialis (MG), and soleus (SOL) were recorded wirelessly from the right leg at 2 kHz (Myon AG, Baar, Switzerland). Before electrode application, the skin at each recording site was shaved, abraded, and cleaned to reduce impedance. Bipolar electrodes (Ag/AgCl; Covidien, Mansfield, MA) were then placed according to SENIAM recommendations, except for SOL, which was placed medial to the muscle belly and parallel to its fiber pennation angle. Each signal was then checked for clarity and strength during an attempted isolated contraction. All cables and electrodes were then secured to the skin using a combination of adhesive tape and self-adhesive bandage to minimize movement artifact.

Data Analysis

Joint power. The 3D motion capture marker trajectories were labeled and exported with all analog data (EMG, crank force and angle) to MATLAB (R2017a; Mathworks Inc., Natick, MA) where they were processed using custom scripts. Crank force signals and marker trajectories were zero-lag low-pass filtered at 12 Hz using a digital second-order Butterworth filter (20). The position (angle) signal collected for the right crank was used to create an antiphase signal, which was used as the angle of the left crank. These angle signals were converted into the global coordinate system and then used to convert the respective crank forces (tangential and radial) into their horizontal and vertical components with respect to the same global coordinate system. These force components, along with the marker trajectories, were then rotated into the ergometer coordinate system using 2D and 3D rotation matrices, respectively. The origin of the resultant force was determined by creating a virtual marker at the center of the cleat attachment. This approximation was determined using the crank angle, 3D shoe orientation, and shoe size and then verified against a second approximation using the bottom bracket position, crank length, crank angle, and pedal spindle length.

Inverse kinematics and inverse dynamics were calculated using OpenSim software (21). First, a previously developed generic full-body musculoskeletal model (22) was scaled to each participant's anthropometry. Segment length of the arms, trunk, and legs were scaled in all three axes using the distance between nominated marker pairs. Scaling factors were calculated by comparing these distances to that of the generic model. The mass of the participant was then used in combination with these scaling factors to distribute segment masses. This scaled model, as well as the kinematic and kinetic data collected during the submaximal trials, was used to run inverse kinematics and inverse dynamics via the Application Programming Interface between OpenSim and MATLAB. The inverse kinematics tool within OpenSim calculates joint angles at each time step by using a weighted least squares fit to minimize errors between the experimental and the model markers. These results are then combined with external loads applied to the model, in this case reaction forces at the left and right crank, to determine the net joint moment at the ankle, knee, and hip joints. Joint power was calculated as the dot product of the net joint moment and joint angular velocity. Flexor moments and flexion velocity were defined as positive. Net joint power was calculated as the mean joint power over a complete crank cycle starting and finishing at top dead center. Total positive and negative power was calculated by taking the mean value only when joint power was positive or negative, respectively (23). Individual joint power contributions to leg power were calculated by dividing individual net joint power by the summed net joint power of the hip, knee, and ankle. Data from the submaximal trials were averaged across five cycles of the right crank where the participant was able to simultaneously match the target power (±5%) and cadence (±5%), except for one participant in the seated trial at 70 rpm, who could only manage two cycles at the target power and cadence. All other data were excluded from the analysis.

Muscle activity. DC offset was removed from the raw EMG signal for each muscle before band-pass filtering between 20 and 400 Hz. The signals were then rectified and low-pass filtered at 15 Hz using a fourth-order zero-lag digital Butterworth filter. The resulting EMG signals were interpolated to 360 data points per cycle to enable a mean signal to be calculated over the same five crank cycles used for the joint power data. The mean signals were then normalized to the peak EMG RMS value from the trial in which the participant achieved $P_{max,i}$. Because of movement artifact, several trials for specific recording sites were discarded. Results for GMax, RF, and VL were averaged across 14 participants, MG and SOL were averaged across 12 participants, and BF was averaged across 10 participants.

EMA. As defined by Biewener (24), "Effective mechanical advantage (EMA) is the ratio of the extensor muscle moment arm (r) to the moment arm of the ground reaction force (R) acting about the joint." In cycling, the reaction force on the crank takes the place of the ground reaction force for this ratio. Hence, closer alignment of the joint center of rotation to the crank reaction force vector will increase a muscle group's EMA. Extensor muscle moment arms (r) of the right hip, knee, and ankle were calculated within OpenSim software using the

moment arms of gluteus maximus as the hip extensor moment arm, vastus lateralis for the knee, and soleus for the ankle. In each condition, EMA values of hip extensors, knee extensors, and ankle plantar flexors were calculated at the time of the peak resultant crank force.

Statistics

A two-way repeated-measures ANOVA was performed to test for main effects of posture and cadence and interaction effects (posture–cadence) on relative joint power, EMA, and mean EMG RMS. The alpha level for main and interaction effects was set at 0.037 before statistical analysis. This alpha level was based on a desired false-positive risk of <5%, a prior probability for a real effect of 0.5, a sample size of 15, and an estimated effect size (ES) of 1 (25). Whenever a main or interaction effect was found, multiple comparisons were used to detect the effect of the factor(s) in each condition. The alpha level was corrected for family-wise multiple comparisons using the Sidak method. As per recommendations (26,27), the F value, P value, and generalized eta-squared (η) are provided for main and interaction effects. For multiple comparisons, the t statistic, adjusted P value, 95% confidence interval (95% CI [low–high]), and corrected ES known as Hedges' g_{av} (ES) are provided. The generalized eta-squared (η^2_G) for each variable was assessed against the benchmarks of trivial (<0.0099), small (0.0099–0.0588), moderate (0.0588–0.1379), and large effect (>0.1379) (28). The corrected ES for each variable was assessed against the commonly used benchmarks of small (0.1–0.3), moderate (0.3–0.5), and large effect (≥0.5) (26). All values are reported as mean ± SD.

RESULTS

The mean $P_{max.i}$ across the participant group was 1605 ± 368 W (21.5 ± 4 W·kg^{-1}), giving a mean power output of 10.74 ± 2 W·kg^{-1} for the submaximal trials. We individualized the mean crank power output over a complete crank cycle for the submaximal trials (10.74 ± 2 W·kg^{-1}) as 50% of each participant's $P_{max.i}$ recorded during the maximal power output test. Thus, the power output for the submaximal trials was approximately equal to 85% of each participant's mean maximal power output ($P_{max.m}$) recorded during the maximal power output test (see Table 1). Furthermore, because of the effect of cadence on maximal power production, it is likely that the submaximal power output was near maximal during the 70-rpm conditions. There was good agreement between the target power and cadence with power and cadence measured at the crank during each submaximal trial, respectively (see Table 1). Group mean crank torque, velocity, and power curves with respect to crank angle during the maximal power output test and submaximal trials have been provided as supplementary information (see Figure, Supplementary Digital Content 1, Participant and group mean crank force, velocity, and power during the maximal power output test as well as a comparison of crank and leg power during the submaximal trials, http://links.lww.com/MSS/B918). There was a clear rightward phase shift in crank resultant force, velocity, and power when nonseated compared with seated, as well as a large difference between crank power and leg power during the downstroke, as has previously been demonstrated (10).

Mean power production at the hip, knee, and ankle with respect to crank angle is shown in Figure 2, from which clear effects of posture and cadence can be seen. At 70 rpm, power curves for all joints are phase shifted to the right when nonseated;

TABLE 1. Group mean ± SD crank power (W·kg^{-1}), cadence (rpm), and joint power (W·kg^{-1}) during the maximal sprint and submaximal trials.

	Maximal Sprint	70 rpm		120 rpm		Two-Way ANOVA (Posture–Cadence)
	Seated	Seated	Nonseated	Seated	Nonseated	Main and Interaction Effects
Cadence	120 ± 2	70 ± 3	71 ± 3	118 ± 4	119 ± 4	No main or interaction effects
Crank power						
Peak instantaneous ($P_{max.i}$)	21.48 ± 3.97	15.67 ± 1.28	17.94 ± 2.12	17.29 ± 2.48	18.34 ± 2.79	(–)
% $P_{max.i}$	100 ± 0	75 ± 12	85 ± 14	81 ± 8	86 ± 10	(–)
Mean						
Both cranks ($P_{max.m}$)	13.52 ± 2.53	11.27 ± 1.45	11.45 ± 1.62	11.23 ± 1.56	11.36 ± 1.50	(–)
% $P_{max.i}$	63 ± 4	53 ± 5	54 ± 6	53 ± 5	54 ± 5	(–)
% $P_{max.m}$	100 ± 0	85 ± 11	86 ± 12	84 ± 9	85 ± 11	(–)
% Target power	(–)	106 ± 11	108 ± 12	106 ± 9	107 ± 10	(–)
Right crank	6.94 ± 0.66	5.67 ± 0.67	5.82 ± 0.86	5.65 ± 0.81	5.74 ± 0.80	Posture (F = 9.5, P = 0.008, η^2_G = 0.006 [trivial])
% Both cranks	51 ± 1	50 ± 1	52 ± 2	50 ± 2	51 ± 2	(–)
Joint power						
Right leg	(–)	4.92 ± 0.34	4.95 ± 0.60	5.47 ± 0.69	5.67 ± 0.69	Cadence (F = 56, P < 0.001, η^2_G = 0.24 [large])
% Right crank	(–)	87 ± 7	86 ± 7	97 ± 7	99 ± 9	(–)
Hip	(–)	2.39 ± 0.80	2.94 ± 0.87	3.62 ± 1.03	4.40 ± 0.99	Posture (F = 37, P < 0.001, η^2_G = 0.12 [moderate]); Cadence (F = 278, P < 0.001, η^2_G = 0.36 [large])
% Right leg	(–)	49 ± 15	59 ± 16	66 ± 18	78 ± 15	(–)
Knee	(–)	1.26 ± 0.71	0.48 ± 0.74	0.89 ± 1.00	0.06 ± 0.86	Posture (F = 80, P < 0.001, η^2_G = 0.20 [large]); Cadence (F = 13, P < 0.003, η^2_G = 0.055 [small])
% Right leg	(–)	26 ± 15	9 ± 15	16 ± 19	1 ± 15	(–)
Ankle	(–)	1.27 ± 0.28	1.53 ± 0.30	0.96 ± 0.32	1.21 ± 0.32	Posture (F = 26, P < 0.001, η^2_G = 0.16 [large]); Cadence (F = 34, P < 0.001, η^2_G = 0.23 [large])
% Right leg	(–)	26 ± 6	31 ± 5	17 ± 5	21 ± 6	(–)
Residual*	(–)	0.81 ± 0.52	0.87 ± 0.49	0.18 ± 0.39	0.07 ± 0.54	(–)
% Right crank	(–)	13 ± 7	14 ± 7	3 ± 7	1 ± 9	(–)

*Residual power was calculated as the difference between right crank power and right leg power, which provides an estimate of the net power contributed by muscles in the upper limbs. NB: Target power for the submaximal trials was 10.74 ± 1.99 W·kg^{-1}. η^2_G, generalized eta-squared; ES, Hedges' g_{av} corrected ES. (–) indicates that either data were not calculated or statistical analysis was not performed.

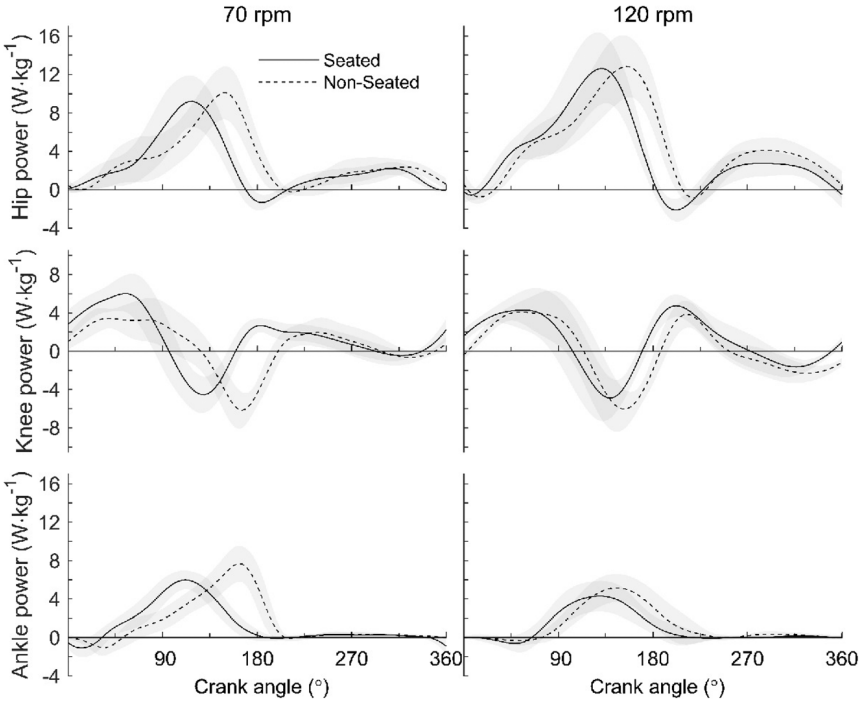

FIGURE 2—Comparison of group mean ± SD (*shaded area*) hip, knee, and ankle power in the right leg between the seated (*solid lines*) and the nonseated (*dashed lines*) postures during very-high-power output cycling at 70 and 120 rpm. NB: Power curves are visibly phase shifted to the right when nonseated, particularly at 70 rpm. Knee power curves are characterized by a significant period of negative power during the downstroke.

however, this phase shift is less pronounced at 120 rpm. In all conditions, the crank cycle begins with power being generated predominantly through knee extension. At 70 rpm, this contribution is much greater in the seated posture, but similar between postures at 120 rpm. The power generation phase at the knee is followed by an absorption phase, which occurs simultaneously with hip extension and ankle plantarflexion power. During this period, the hip contributes significantly more power at 120 rpm than at 70 rpm. At 70 rpm, the ankle begins the crank cycle with a small period of negative plantarflexion power in both postures, after which its positive power steadily increases. Positive power contributions at the hip and knee during the second half of the crank cycle are clearly visible.

All statistics (F, P, η^2_G, t statistic, adjusted P value, 95% CI [low–high], and corrected ES) relating to the effects of posture and cadence on crank power, cadence, and joint power contributions are provided in Table 1. This analysis revealed the main effects of posture on net joint power contributions, which resulted in a moderate increase in hip power, a large decrease in knee power, and a large increase in ankle power in the nonseated compared with seated posture (Fig. 3A). At both cadences, knee power in the nonseated posture was 15% (~0.8 W·kg^{-1}) less than when seated. At 70 rpm, hip power increased by 10% (0.55 W·kg^{-1}) and ankle power by 5% (0.26 W·kg^{-1}) in the nonseated compared with seated posture. At 120 rpm, hip power increased by 12% (0.78 W·kg^{-1}) and ankle power by 4% (0.25 W·kg^{-1}) in the nonseated compared with seated posture. Interestingly, net knee power was lower than net hip and ankle power in all conditions. There was also a main effect of cadence on the power contributed at each joint, which resulted in a large increase in hip power, a small decrease in knee power, and a large decrease in ankle power when cycling at 120 rpm compared with 70 rpm (see Table 1).

The contribution of each joint to both positive and negative power is shown in Figure 3B–D. In all conditions, the knee contributed positive power in the first and third quarters of the crank cycle; however, this was offset by large amounts of negative power during the second quarter. There was a 21.5% increase in negative power during knee extension when nonseated (−0.8 W·kg^{-1}) compared with seated (−0.6 W·kg^{-1}) at 70 rpm and a 22.4% increase in negative power during knee extension when nonseated (−0.9 W·kg^{-1}) compared with seated (−0.7 W·kg^{-1}) at 120 rpm. Hip flexion power accounted for 24% ± 6% (1.1 W·kg^{-1}) of positive hip power when nonseated at 120 rpm compared with 20% ± 9% (0.8 W·kg^{-1}) when seated. When seated at 70 rpm, knee flexion power accounted for 32% ± 8% (0.6 W·kg^{-1}) of positive knee power compared with 27% ± 13% (0.4 W·kg^{-1}) when nonseated. At 120 rpm, knee flexion power accounted for 44% ± 11% (0.8 W·kg^{-1}) of positive knee power compared with only 34% ± 10% (0.5 W·kg^{-1}) when nonseated.

An unsurprising but noteworthy result was the discrepancy in power between the ergometer, cranks, and legs. Power measured at the crank was marginally greater than power measured by the ergometer, which was likely due to power losses in the drivetrain. Leg power was significantly lower than crank power in both postures at 70 rpm but not at 120 rpm, likely due to power being contributed at the crank by body mass and muscles within the arms and torso. There was a main effect of cadence on leg power, which resulted in a significant increase in leg power at 120 rpm compared with 70 rpm. At 70 rpm, leg power

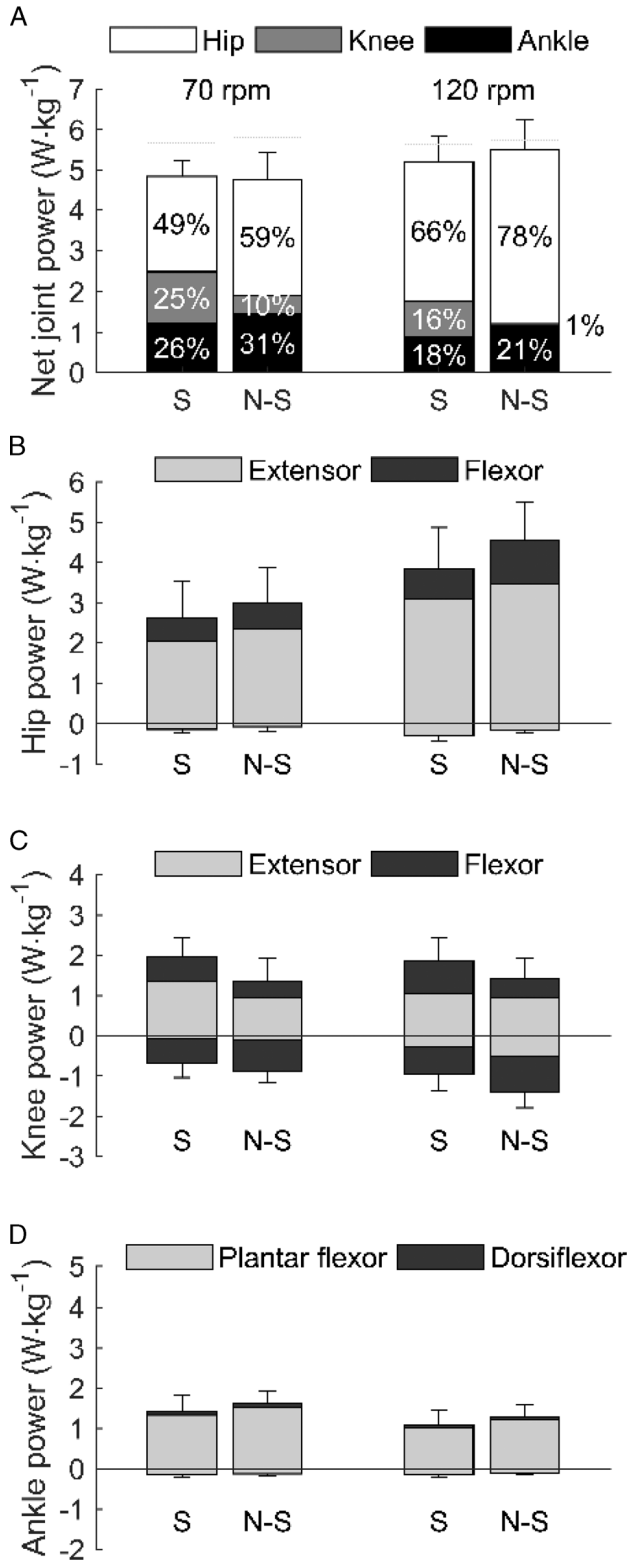

FIGURE 3—A, Leg power (mean ± SD) per cycle in the seated (S) and nonseated (N-S) posture during very-high-power output cycling at 70 and 120 rpm. Stacked bars show the net power contribution (%) at the hip, knee, and ankle to leg power. The breakdown of joint power into positive and negative contributions during net flexor and extensor muscle moments is shown for the hip (B), knee (C), and ankle (dorsiflexor/ plantar flexor) (D). NB: The reduction in net knee power is the result of large amounts of positive and negative power at the knee.

accounted for 86% ± 7% of crank power when nonseated and 87% ± 7% when seated. At 120 rpm, leg power accounted for 99% ± 9% when nonseated and 97% ± 7% when seated. Previous research (13) has shown that muscle activity within the upper limbs and forces at the handlebar increase significantly during high-power output cycling. Thus, it seems plausible that greater contributions of power from upper body mass and muscles within the arms and torso occur when higher crank force is required, especially when in the nonseated posture.

EMA at the knee was significantly greater when nonseated compared with seated at the time of peak resultant crank force production ($F = 103$, $P < 0.001$, $\eta^2_G = 0.27$ [large]) (Fig. 4). The moderate interaction effect between posture and cadence ($F = 9.4$, $P = 0.008$, $\eta^2_G = 0.1$) meant that the increase in EMA at the knee when nonseated was greater at 70 rpm (seated = 0.34 ± 0.09 vs nonseated = 0.52 ± 0.15, $t = 6.1$, $P < 0.001$, 95% CI = 0.1–0.3, ES = 1.4 [large]) than at 120 rpm (seated = 0.29 ± 0.07 vs nonseated = 0.35 ± 0.08, $t = 3.5$, $P = 0.004$, 95% CI = 0.02–0.1, ES = 0.7 [Large]). In both postures, there was a moderate increase in EMA at the hip ($F = 8.9$, $P = 0.01$, $\eta^2_G = 0.08$) and a small decrease in EMA at the ankle ($F = 17$, $P = 0.001$, $\eta^2_G = 0.04$) at 70 rpm compared with 120 rpm.

BF was the only muscle to show a main effect of posture on mean EMG RMS (Fig. 5). At both cadences, there was a large decrease in BF activity in the nonseated compared with seated posture ($F = 92$, $P < 0.001$, $\eta^2_G = 0.6$). Predictably, the mean EMG RMS signal of all muscles was higher at 70 rpm than at 120 rpm ($P < 0.001$) because of the increase in torque required to maintain the set power output, which was likely to be closer to a quasi-maximal power output for each participant at the cadence of 70 rpm (16,17).

Statistical analysis was also performed on the magnitude and timing of peak joint angles, velocities, and moments (see Table, Supplemental Digital Content 2, which summarizes the significant main and interaction effects of posture and cadence, http://links.lww.com/MSS/B919). Of note is the 0.33-N·m·kg^{-1} reduction in the peak knee extension moment when nonseated at 70 rpm and the significant increase in peak knee extension angle when nonseated at 70 rpm (~9°) and 120 rpm (~12°) compared with when seated. Angular displacement, velocity, and moments at the hip, knee, and ankle with respect to crank angle have also been provided (see Figures, Supplemental Digital Content 3–5, group mean [i] joint angle curves of the hip, knee, and ankle; [ii] joint velocity curves of the hip, knee, and ankle; and [iii] joint moment curves of the hip, knee, and ankle, respectively, http://links.lww.com/MSS/B920, http://links.lww.com/MSS/B921, and http://links.lww.com/MSS/B922) as well as EMG RMS signals with respect to crank angle (see Figure, Supplemental Digital Content 6, group mean EMG RMS envelopes of GMax, BF, RF, VL, MG, and SOL, http://links.lww.com/MSS/B923).

DISCUSSION

The aim of this experiment was to compare power production across the hip, knee, and ankle between seated and

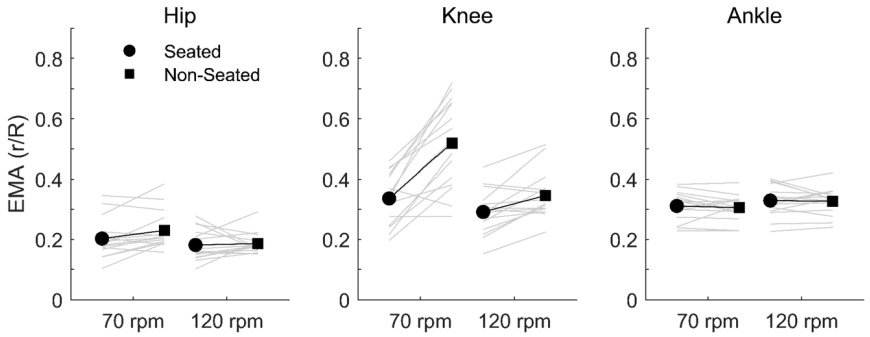

FIGURE 4—EMA of the hip, knee, and ankle at the time of peak resultant crank force production in the seated (S) and nonseated (N-S) posture during very-high-power output cycling at 70 and 120 rpm. Data for each participant (*gray lines*) are shown along with the group mean (*black lines*).

nonseated cycling postures. This comparison was made when cycling at a very-high-power output (above the reported seated to nonseated threshold) at two different cadences (70 and 120 rpm). The results support our primary hypothesis that joint power would be distributed away from the knee joint when cycling in a nonseated posture compared with when seated. In partial support of our second hypothesis, the redistribution of knee power due to the change in posture was different at each cadence; however, it was not redistributed solely to the hip and ankle as we predicted. Cycling in a nonseated posture at 70 rpm resulted in 14% of crank power being redistributed away from the knee to the hip (+8%) and ankle (+4%) compared with when seated. Cycling in a nonseated posture at 120 rpm resulted in 15% of crank power being redistributed away from the knee to the hip (+13%) and ankle (+4%) compared with when seated. The discrepancy between the change in knee power relative to hip and ankle power suggests that there was a net gain in upper body power when cycling in a nonseated compared with seated posture at 70 rpm and a net loss in upper body power when cycling in a nonseated posture at 120 rpm compared with when seated. Cycling in a nonseated posture at 70 rpm also appears to increase the effectiveness of ankle power production, as higher levels of ankle power were produced without an increase in plantar flexor (MG and SOL) activity. At 120 rpm, hip power increased using similar levels of muscle activation in GMax and RF as at 70 rpm, but with lower levels of activation in BF, which may indicate that cyclists are more effective at producing hip power when in the nonseated posture.

A key result of this study was that the nonseated posture increased negative power at the knee, which resulted in decreased net power at the knee. The increase in negative knee power, while the knee was extending, provides evidence that greater amounts of knee extension power are transferred away from the knee joint when nonseated. It is well understood that the coordinated activity of mono- and biarticular muscles can serve to transfer energy across joints and orient the crank reaction force

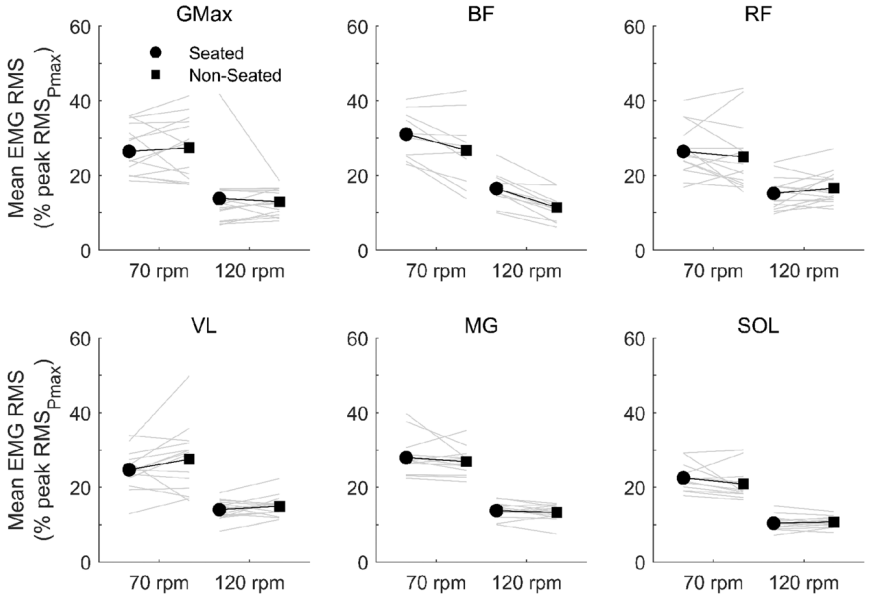

FIGURE 5—Mean muscle activity (EMG RMS across the crank cycle, normalized to each muscle's peak RMS activity during the maximal power output test) for the gluteus maximus (GMax), rectus femoris (RF), biceps femoris (BF), vastus lateralis (VL), medial gastrocnemius (MG), and soleus (SOL) in the seated (S) and nonseated (N-S) posture during very-high-power output cycling at 70 and 120 rpm. NB: Because of the increase in torque required per crank cycle, muscle activity was significantly greater at 70 and 120 rpm for all muscles. Data for each participant (*gray lines*) are shown along with the group mean (*black lines*).

during the downstroke (29). In light of this, it is important to note the individual muscle-joint designs of BF and MG (30,31). For example, BF's moment arm is larger at the hip than at the knee, which means that co-contraction of VL and BF can transfer knee extension power to the hip. MG's moment arm is larger at the ankle than at the knee, which means co-contraction of VL and MG can transfer knee extension power to the ankle. Thus, shifting to a nonseated posture appears to use the ability of BF and MG to transfer knee extension power to the hip and ankle, respectively.

In line with previous research (32), joint moments at the hip, knee, and ankle were significantly altered by the change in posture, which suggests that transitioning to the nonseated posture when high crank forces are required can provide significant mechanical benefits. When nonseated at 70 rpm, peak extension moments at the hip, knee, and ankle contributed to the resultant crank force being more closely aligned to the knee joint center. As such, EMA at the knee was 53% higher in the nonseated posture (0.52 ± 0.15) compared with when seated (0.34 ± 0.09) at 70 rpm. Net torque requirements at the knee were reduced when nonseated; however, mean RMS activity of the knee extensors (VL and RF) was similar between postures. Given the cautious assumption that the measured EMG in VL and RF provides an indication of the active muscle volume within the knee extensors (33), it appears that when in the nonseated posture, riders were able to support their bodyweight while also fulfilling the external power requirement at the cranks using a similar active volume of knee extensor muscle.

It may also be the case that switching to a nonseated posture at 70 rpm increases the force-producing capability of knee extensor muscles. The peak knee extension angle and range of motion increased significantly in the nonseated posture; however, the increased range of motion did not lead to an increase in the mean extension velocity. This is because a greater portion of the crank cycle was spent extending the knee. For example, when nonseated at 70 rpm, the period of knee extension was so great (59%) that the mean knee extension velocity was actually 5.8% lower than when seated. As supported by the findings of Brennan et al. (34), the reduction in mean knee extension velocity in the nonseated ($181°\cdot s^{-1}$) compared with seated ($192°\cdot s^{-1}$) posture at 70 rpm would bring the fascicle shortening velocity of VL closer to its optimum for both efficiency and force production. Thus, it appears that riders use extra degrees of freedom afforded in the nonseated posture to increase the force-producing capabilities of knee extensor muscles.

Power generated during hip flexion and knee flexion played a critical role in the differences in positive hip and knee power between postures. Interestingly, when in the nonseated posture at 120 rpm, almost half of the 12% increase in the contribution of positive hip power was due to hip flexion power. We only measured the activity of one hip flexor muscle (RF), making it difficult to provide insight into this finding as other hip flexor muscles such as iliacus, psoas, and sartorius were likely responsible for this increase. At both cadences, a large portion of the 15% increase in positive knee power when seated compared with nonseated was due to knee flexion power. The increase in knee flexion power was not reflected by any difference in BF activity during the period of knee flexion power production between postures. Thus, the most likely explanation is other knee flexor muscles were responsible for this increase. Another explanation is the greater mean knee flexion angle when seated compared with nonseated may have shifted the fascicle operating lengths of the knee flexors closer to optimal and hence been more favorable for generating power (34). On the whole, it appears there is a greater reliance on knee flexors to contribute power when seated, and there is a greater reliance on hip flexors to produce power when nonseated at 120 rpm.

The limitations inherent to inverse dynamics (35,36) and quantifying surface EMG (33) must be acknowledged when attempting to understand function and performance from an energetic perspective. One must consider that individual muscle force and power contributions cannot be inferred from joint-level analyses, nor can the level of neural drive to muscle be fully inferred from surface EMG. A further limitation pertains to the questionable ecological validity of ergometer cycling because of the constraint of frontal plane bicycle dynamics (37). It has been shown that when cycling in a nonseated posture in the field, cyclists sway the bike laterally underneath their body (38), which might affect the power generating profile of different joints. Finally, accurate conclusions were unable to be made about which technique would be more economical, as metabolic cost (oxygen consumption) was not measured. However, because of the very-high-power output and short duration of the conditions tested here, it is unlikely that the rate of metabolic energy expenditure with respect to time or per unit distance was the variable being optimized in either posture.

In summary, the contribution of knee joint power to total leg power was reduced by switching from a seated to nonseated posture during very-high-power output cycling. The decrease in net knee power when in the nonseated posture is likely the result of power produced by knee extensors being transferred by biarticular muscles to the hip and ankle. This coordination strategy and increase in EMA at the knee joint means it is likely that both nonmuscular and muscular power is more effectively transferred to the crank compared with when seated. These results highlight important differences in joint power contributions during seated and nonseated cycling, which may be a fundamental aspect of why cyclists choose to frequently use a nonseated posture when needing to produce very high levels of crank torque and power.

Ross D. Wilkinson was supported by an Australian Government Research Training Program Scholarship.

The authors report no conflicts of interest. The results of the present study do not constitute endorsement by the American College of Sports Medicine. The results of the study are presented clearly, honestly, and without fabrication, falsification, or inappropriate data manipulation.

REFERENCES

1. Costes A, Turpin NA, Villeger D, Moretto P, Watier B. A reduction of the saddle vertical force triggers the sit–stand transition in cycling. *J Biomech*. 2015;48(12):2998–3003.
2. Hansen EA, Waldeland H. Seated versus standing position for maximization of performance during intense uphill cycling. *J Sports Sci*. 2008;26(9):977–84.
3. Stone C, Hull ML. Rider/bicycle interaction loads during standing treadmill cycling. *J Appl Biomech*. 1993;9:202–18.
4. Caldwell GE, Li L, McCole SD, Hagberg JM. Pedal and crank kinetics in uphill cycling. *J Appl Biomech*. 1998;14(3):245–59.
5. Stone C, Hull ML. The effect of rider weight on rider-induced loads during common cycling situations. *J Biomech*. 1995;28(4):365–75.
6. Millet GP, Tronche C, Fuster N, Candau R. Level ground and uphill cycling efficiency in seated and standing positions. *Med Sci Sports Exerc*. 2002;34(10):1645–52.
7. Reiser RF 2nd, Maines JM, Eisenmann JC, Wilkinson JG. Standing and seated Wingate protocols in human cycling. A comparison of standard parameters. *Eur J Appl Physiol*. 2002;88:152–7.
8. Poirier E, Do M, Watier B. Transition from seated to standing position in cycling allows joint moment minimization. *Sci Sports*. 2007; 22:190–5.
9. Vandewalle H, Peres G, Heller J, Panel J, Monod H. Force-velocity relationship and maximal power on a cycle ergometer. Correlation with the height of a vertical jump. *Eur J Appl Physiol Occup Physiol*. 1987;56:650–6.
10. Elmer SJ, Barratt PR, Korff T, Martin JC. Joint-specific power production during sub-maximal and maximal cycling. *Med Sci Sports Exerc*. 2011;43(10):1940–7.
11. McDaniel J, Behjani NS, Elmer SJ, Brown NA, Martin JC. Joint-specific power–pedaling rate relationships during maximal cycling. *J Appl Biomech*. 2014;30:423–30.
12. Li L, Caldwell GE. Muscle coordination in cycling: effect of surface incline and posture. *J Appl Physiol*. 1998;85(3):927–34.
13. Turpin NA, Costes A, Moretto P, Watier B. Upper limb and trunk muscle activity patterns during seated and standing cycling. *J Sports Sci*. 2017;35(6):557–64.
14. Tanaka H, Bassett DR Jr, Best SK, Baker KR Jr. Seated versus standing cycling in competitive road cyclists: uphill climbing and maximal oxygen uptake. *Can J Appl Physiol*. 1996;21(2):149–54.
15. Harnish C, King D, Swensen T. Effect of cycling position on oxygen uptake and preferred cadence in trained cyclists during hill climbing at various power outputs. *Eur J Appl Physiol*. 2007;99:387–91.
16. Gardner AS, Martin JC, Martin DT, Barras M, Jenkins DG. Maximal torque- and power-pedaling rate relationships for elite sprint cyclists in laboratory and field tests. *Eur J Appl Physiol*. 2007;101(3): 287–92.
17. Dorel S, Hautier CA, Rambaud O, et al. Torque and power–velocity relationships in cycling: relevance to track sprint performance in world-class cyclists. *Int J Sports Med*. 2005;26:739–46.
18. Dorel S. Maximal force–velocity and power–velocity characteristics in cycling: assessment and relevance. In: Morin J-B, Samozino P, editors. *Biomechanics of Training and Testing: Innovative Concepts and Simple Field Methods*. Cham: Springer International Publishing; 2018. pp. 7–31.
19. Lucia A, Hoyos J, Chicharro JL. Preferred pedalling cadence in professional cycling. *Med Sci Sports Exerc*. 2001;33(8):1361–6.
20. Kristianslund E, Krosshaug T, Van den Bogert AJ. Effect of low pass filtering on joint moments from inverse dynamics: implications for injury prevention. *J Biomech*. 2012;45(4):666–71.
21. Delp SL, Anderson FC, Arnold AS, et al. OpenSim: open-source software to create and analyze dynamic simulations of movement. *IEEE Trans Biomed Eng*. 2007;54(11):1940–50.
22. Rajagopal A, Dembia CL, DeMers M, Delp DD, Hicks JL, Delp SL. Full-body musculoskeletal model for muscle-driven simulation of human gait. *IEEE Trans Biomed Eng*. 2016;63(10):2068–79.
23. Winter DA. Mechanical work, energy, and power. In: *Biomechanics and Motor Control of Human Movement*. 4th ed. 2009. pp. 139–75.
24. Biewener AA. Scaling body support in mammals: limb posture and muscle mechanics. *Science*. 1989;245(4913):45–8.
25. Longstaff C, Colquhoun D. False Positive Risk Web Calculator, version 1.6 [Internet]. [cited 2017 Feb 11]. Available from: http://fpr-calc.ucl.ac.uk/.
26. Bakeman R. Recommended effect size statistics for repeated measures designs. *Behav Res Methods*. 2005;37(3):379–84.
27. Lakens D. Calculating and reporting effect sizes to facilitate cumulative science: a practical primer for t-tests and ANOVAs. *Front Psychol*. 2013;4:863.
28. Albers C, Lakens D. When power analyses based on pilot data are biased: inaccurate effect size estimators and follow-up bias. *J Exp Soc Psychol*. 2018;74:187–95.
29. Dorel S. Mechanical effectiveness and coordination: new insights into sprint cycling performance. In: Morin J-B, Samozino P, editors. *Biomechanics of Training and Testing: Innovative Concepts and Simple Field Methods*. Cham: Springer International Publishing; 2018. pp. 33–62.
30. Lieber RL, Ward SR. Skeletal muscle design to meet functional demands. *Philos Trans R Soc Lond B Biol Sci*. 2011;366:1466–76.
31. Kuo AD. The action of two-joint muscles: the legacy of W.P. Lombard. In: *Classics in Movement Science*. Champaign (IL): Human Kinetics; 2001. pp. 289–315.
32. Caldwell GE, Hagberg JM, McCole SD, Li L. Lower extremity joint moments during uphill cycling. *J Appl Biomech*. 1999;15:166–81.
33. Enoka RM. *Neuromechanics of Human Movement*. 4th ed. Champaign (IL): Human Kinetics; 2008. pp. 197–204.
34. Brennan SF, Cresswell AG, Farris DJ, Lichtwark GA. The effect of cadence on the mechanics and energetics of constant power cycling. *Med Sci Sports Exerc*. 2019;51:941–50.
35. Zelik KE, Kuo AD. Mechanical work as an indirect measure of subjective costs influencing human movement. *PLoS One*. 2012; 7(2):e3114.
36. Hicks JL, Uchida TK, Seth A, Delp SL. Is my model good enough? Best practices for verification and validation of musculoskeletal models and simulations of movement. *J Biomech Eng*. 2015;137: 020905.
37. Cain SM, Ashton-Miller JA, Perkins NC. On the skill of balancing while riding a bicycle. *PLoS One*. 2016;11(2):e0149340.
38. Soden PD, Adeyefa BA. Forces applied to a bicycle during normal cycling. *J Biomech*. 1978;12:527–41.